Published in final edited form as:
Org Biomol Chem. 2013 January 7; 11(1): 69–77. doi:10.1039/c2ob26445e.

Positional effects of click cyclization on β-hairpin structure, stability, and function†

Jessica H. Park and **Marcey L. Waters***
Department of Chemistry, CB 3290, University of North Carolina, Chapel Hill, NC, 27599, USA.

Abstract

The use of the copper (I)-assisted azide-alkyne cycloaddition (CuAAC, or "click" reaction) as a method of β-hairpin stabilization was investigated at several different positions to determine the impact on hairpin structure and function, including hydrogen bonded sites, non-hydrogen bonded sites, and at the peptide termini. The role of the turn sequence in the peptide and the chain length of the azied were also investigated. It was determined that the CuAAC reaction was a suitable method for locking in β-hairpin structure in peptides possessing either the type I' turn, VNGO and the type II' turn, VpGO. Moreover, all cyclic variants exhibited improved thermal stability and resistance to proteolysis as compared to the non-cyclic peptides, regardless of the position in the strand. Additionally, the function of the CuAAC cyclized peptides was not altered as exhibited by similar binding affinities for ATP as the WKWK peptide. These studies provided a comprehensive method for CuAAC cyclization of β-hairpin peptides, which could further be utilized in the inhibition of protein-protein and protein-nucleic acid interactions.

Introduction

While small molecules are optimal for inhibition of enzymes, they have been less successful at the inhibition of interactions between two biomolecules, such as protein-protein, protein-DNA, and protein-RNA interactions. These interactions play a critical role in many disease states, such as the p53-HDM2 interaction in cancer[1], sirtuin1 and PGC1-α in diabetes[2], and CRP and PINK1 in atherosclerosis[3] as examples of dysregulated protein-protein interactions, and the binding of TAR RNA by the TAT protein interaction as an example of a medicinally relevant protein-RNA interaction. For this reason, researchers have sought to mimic the interface of PPIs and protein-nucleic acid interactions to disrupt the protein contacts, thereby inhibiting or slowing the progression of disease. One approach to mimic the interface is to excise the hotspot of a protein, the group of amino acids at the intermolecular protein interface that contribute to most of the binding energy.[4] However, it is well known that isolation of a small portion of a protein often leads to an unfolded peptide, and random coil peptides are susceptible to rapid enzymatic degradation. In addition, the lack of structure often renders the peptide nonfunctional. To this end, there is a

†Electronic Supplementary Information (ESI) available: See DOI: 10.1039/b000000x/

mlwaters@unc.edu; Fax: 919-962-2388; Tel: 919-843-6522.

necessity to provide methods of stabilization of the structure as well as to minimize proteolytic degradation and maintain functionality.

A significant amount of research has been accomplished in stabilizing peptide secondary structural motifs. Several groups report the use of chemical methods that are high-yielding to stabilize α-helices through intramolecular side-chain reactions.[5] Moellering et al. utilized ring closing metathesis (RCM) on the dnMAML1 to stabilize its α-helical structure and prove its ability to inhibit the Notch signaling pathway.[6] While Arora's group employed RCM to afford a hydrogen bond surrogate in the backbone of an α-helical portion of HIF-1α to inhibit p300.[7] Klaveness and Bong have used copper (I)-assisted azide-alkyne cycloaddition (CuAAC or "click' cyclization)[8] to stabilize 3,10-helices[9] and α-helices[5b], respectively. More recently CuAAC has been used as a method to replace disulfide linkages in an antibiotic, Tachyplesin I, which retained biological activity.[10] In addition, Celentano et al. have performed studies with a TrpZip peptide to incorporate the 1,4-triazole linkage in the non-hydrogen bonded site of a β-hairpin.[11]

A common method for β-hairpin stabilization is cyclization via amide bond formation through the backbone or side chains.[12] However, these approaches are labor intensive and often low yielding. In cases where a library of cyclic peptides is warranted, as in Robinson's approach to disrupting protein-RNA and protein-protein interactions with cyclic β-hairpins,[13] an alternate method of cyclization would be advantageous.

Herein, we report a comprehensive study of the impact of "click" cyclization on β-hairpin structure and function through variation of the position of triazole incorporation in the hairpin, the relative positions of azide and alkyne in the N- and C-terminal strands of the hairpin, the turn sequence, and the chainlength of the azido amino acid. We find that while there are some variations in stability, click cyclization is a general method to stabilize and in some cases enhance the structure of β-hairpins with the incorporation of a 1,4-triazole, regardless of position in the peptide, turn, or chainlength. We chose to utilize mutants of a well-studied β-hairpin peptide, WKWK (Fig 1), to gain insights not only for structural advantages but also impacts on function as this peptide was found to bind ATP.[14] This study not only demonstrates the structural advantages of the CuAAC in β-hairpins but also the preservation of function and enhanced protection to proteolysis. Thus, CuAAC cyclization[15] of β-hairpins is a general and promising approach to the disruption of protein-protein and protein-nucleic acid interactions.

Results

System Design

A series of β-hairpin peptides were designed based on the WKWK peptide to determine the effects of cyclizing via CuAAC on structure and function (Fig 1). The WKWK peptide was chosen as it has been thoroughly characterized and has been shown to be well folded. Additionally, it is known to bind purine bases, specifically ATP with a K_d of 170 μM (Fig 2).[14] Thus, click cyclization of variants of this sequence will allow us to investigate the impact on function as well as structure. The two unnatural amino acids used for the CuAAC cyclization were azidolysine (Azk) and propargylglycine (Pra). Azidolysine is easily

synthetically accessible and allows for flexibility in the cyclic hairpin. These residues were incorporated cross-strand from each other, with Azk in the N-terminal strand and Pra in the C-terminal strand, along the β-hairpin in the hydrogen bonded (HB) positions, non-hydrogen bonded (NHB) positions, and terminal (Term) positions (Fig1, Table I) to investigate positional effects of the click cyclization on β-hairpins. In the HB position, Azk and Pra make two cross-strand hydrogen bonds which rigidify these positions. In the NHB positions, the Azk and Pra residues do not form any hydrogen bonds, giving the sidechains more flexibility. Additionally the positions of Azk and Pra were reversed, such that Pra was in the N-terminal strand and Azk was in the C-terminal strand, to determine any changes in structure. These peptides are denoted with the suffix "rev" (Table I). The effect of the turn sequence was also investigated for all positions by replacing the type I' VNGO turn in WKWK with the type II' VpGO turn. Each peptide was characterized by TOCSY and NOESY 2D NMR and circular dichroism (CD). Peptide stability was evaluated via variable temperature CD studies and protease degradation. Binding was assessed via fluorescence quenching of the Trp residues for applicable peptides.

Structural Studies of the Clicked β-hairpins

Circular Dichroism and 2-D NMR Studies—Structural studies were performed on all uncyclized (denoted by the suffix "U") and cyclic peptides (denoted by the suffix "C") via circular dichroism (CD) and 2-D NMR techniques including TOCSY and NOESY, to assess the influence of cyclization by CuAAC on structure. The β-sheet structure is characterized by a global minimum between 210 nm and 215 nm with a corresponding maximum at 195 nm. A random coil peptide is expected to have a global minimum at 195 nm. 2-D TOCSY and NOESY NMR spectra were acquired on all peptide variants. Downfield shifting of ≥ 0.1 ppm of the α-hydrogens (Hα) along the peptide backbone relative to unfolded values indicates a β-sheet conformation. The NOESY spectra were used to determine proper folding registry in the hairpin and additional interactions between residues.

Terminal Positions for Cyclization—The CD spectrum (Fig 3A) of Term-U and Term-rev-U show a minimum at 212 nm and maximum at 195 nm, distinctive of a global β-hairpin conformation. The cyclic counterparts, Term-C and Term-rev-C exhibit a more intense minimum at the same wavelength suggesting an overall more structured hairpin. Additional confirmation of proper structure is seen with the exciton coupling peak at 225 nm stemming from diagonal Trp interactions which is also seen in the WKWK parent peptide.[14] The NMR data show that non-cyclic and cyclic Term and Term-rev do not display a distinct change in Hα shifts (Fig 3B). The extent of splitting of the diastereotopic Hα's of Gly correlates with hairpin folding at the turn.[15] Both non-cyclic and cyclic peptides of Term and Term-rev have a glycine splitting value of 0.74 ppm, indicating no drastic change in hairpin folding. This lack in difference is most likely due to the position of the CuAAC. There are several aspects to note in comparing the Hα shifts of the non-cyclic and cyclic peptides. Azk, at position -1 or 14, and Pra, at position 13 or -1, are more downfield shifted in the Term-C and Term-rev-C, respectively, suggesting the ends are pulled closer together. Other terminal positions are also stabilized as seen by the downfield shifts of Arg1Hα and Gln12Hα compared to the parent WKWK. Interestingly there is a slight difference in the reversal of the azide and alkyne (Term-rev) which is notable in the shift of Lys11Hα. In WKWK, the

Lys11Hα is upfield shifted stemming from ring current effects from the cross-strand Trp2. This same trend is seen in Term-U, however upon cyclization Lys11Hα is upfield shifted whereas the the reverse trend is seen in Term-rev. This suggests that there are slight nuances in choosing which strand the CuAAC functional groups are placed. Residues surrounding the CuAAC functional groups can certainly impact the structure as is supported by the NOE data (Fig 4). One of the Lys11Hγ of Term-C has a strong NOE with the triazole proton indicating that the presence of the triazole aromatic ring allows Lys11 to have another interaction. This conformation could be inaccessible in the Term-rev-C peptide, thus the downfield shifting is seen as in WKWK.

There are strong NOEs between the Lys4Hα and Trp9Hα, and Lys11Hα and Trp2Hα confirming the correct registry for the β-hairpin. Additional NOE contacts are seen between the side chains of Lys4 and Lys11 and their cross-strand Trp residues, Trp2 and Trp9. However, there is not a significant increase in the contacts between strands upon CuAAC hairpin cyclization. Similar trends were observed in the peptides with a type II' turn sequence, Term-pG (SI Fig S3 & S4). Overall cyclization at the terminal position does not appear to enhance β-hairpin formation dramatically. In addition, there does not appear to be a marked difference in decreasing the number of methylene spacers in the azide residue, from 4 to 3 to 2 to 1, making the loop smaller, (SI Fig S5).

Non-hydrogen bonded position for cyclization—Replacement of the Trp2 and Lys11 cross-strand pair in a non-hydrogen bonded position deters β-hairpin folding since one of the stabilizing Trp-Lys pairs seen in WKWK is removed. This is also apparent in the CD of NHB-U (Fig 5A). The CD spectrum of NHB-U has two minima, one at 205 nm and the other at 215 nm with a maximum at 195 nm suggesting a partially folded structure. NHB-rev-U was not fully soluble and formed a gel-like substance under the same conditions (50 mM KD_2PO_4, pH 7, 20°C) and required a much lower pH to attain solubility. Thus a CD spectrum was not acquired. This again supports the fact that position of the CuAAC functional groups is important. NHB-C and NHB-rev-C both show more hairpin conformation as seen by the sharp decrease in ellipticity at 215 nm. There is a slight shoulder at 205 nm suggesting some population of an unknown structure as seen in NHB-U. The difference in Hα shifts (Fig 5B) agrees with the CD data. Most of the residues in the cyclic peptides display greater downfield shifting than that of the non-cyclic peptides. The glycine splitting values are also far greater for the cyclic peptides at 0.72 ppm and 0.71 ppm relative to 0.63 ppm and 0.55 ppm for NHB and NHB-rev. It appears that covalent linkage at the non-hydrogen bonded site restores stability provided by noncovalent interactions in WKWK. Additionally for NHB-rev, cyclizing restored solubility. The NOESY spectra (Fig 6) better display the structural details of this peptide set. For NHB-U a strong NOE is observed between Lys4Hα and Trp9Hα confirming correct registry, however there is no NOE seen between Azk2 and Pra11. There are additional contacts between the side chains of Lys4 and Trp9. The NOE between Trp9H4 with Val3Hα implies that Trp9 is sandwiched Azk2 and Lys4. NHB-C is also in the correct registry thus showing that click cyclization in the non-hydrogen bonded position does not alter the type of hairpin formed. The sandwiching of Trp9 is far more pronounced in NHB-C as evidenced by NOEs present between Trp9H4 and the methylenes of Azk2. NHB-rev-U does not have any cross-strand

backbone NOEs, suggesting that a β-hairpin is not formed. Instead there is a strong NOE between Azk11Hα and Trp9Hα. Even upon click cyclization no cross-strand NOEs are seen to confirm the correct registry (Fig 6C&D). However, there are strong NOEs observed between Pra2Hα and Lys4Hα as well as between Trp9Hα and Azk11Hα. Structurally the observable NOEs imply a cradling of the hairpin where the terminal ends are sandwiched on top of the residues closer to the turn. NOEs between Trp9 and Lys4 as well as the triazole proton support this structure. Click cyclization at the NHB position of the peptide with the type II' turn, NHB-pG, displayed similar results in the NOEs (SI Fig S7). However, the difference between the CD and Hα shifts of the non-cyclic and cyclic NHB-pG were less pronounced than the type I' turn peptides (SI Fig S6). From these data we conclude that click cyclizing at the non-hydrogen bonded position does indeed stabilize hairpin structure, but with possible distortion.

Hydrogen bonded position for cyclization—The CD spectra of the HB-U and HB-rev-U peptides (Fig 7A) have a broad minimum spanning from 200 nm to 218 nm. Click cyclization for both HB and HB-rev stabilizes a β-hairpin structure as evidenced by a sharp minimum at 215 nm. Exciton coupling at 225 nm from the diagonal Trp2 and Trp9 interaction also confirms the formation of a β-hairpin. The difference in Hα shifts relative to random coil values agree with the CD as nearly all the Hα's in the cyclic peptides exhibit more downfield shifting than the non-cyclic peptides. Additionally the glycine splitting values for HB-U and HB-rev-U increase from 0.48 ppm and 0.59 ppm to 0.66 ppm to 0.69 ppm, respectively, upon triazole formation. This implies that the peptides become more well-folded. Again there are some nuances upon flipping of the click functional groups apparent in Lys4Hα and Lys11Hα (Fig 7B). In the parent WKWK peptide the Lys4Hα is seen to be upfield shifted relative to random coil while Lys11Hα is downfield shifted. HB-U and HB-C both share the same trend as WKWK (Fig 7); however, in HB-rev the trend is reversed where Lys4Hα is downfield shifted and Lys11Hα is upfield shifted. NOEs (Fig 8) provide additional insight into the structural impacts of click cyclization. In both cases NOEs are seen between cross-strand Trp and Lys residues to indicate proper strand registry. HB-rev has several NOEs between crosstrand Trp and Lys pairs as well as additional contacts between Trp and other protons. There is a significant increase in the number of NOEs seen between side-chains upon click cyclization. As with the Term and NHB positions, substitution of the turn residues to the type II' turn, dPro-Gly, sequence in the HB peptide lead to similar results (SI Fig S8 & S9).

Thermal stability of click cyclized β-hairpins

The thermal stability of the peptides was assessed by thermal denaturation monitored by circular dichroism. No direct measurement of melting temperature could be made as no standard S-curve was observed. Nonetheless, in all positions the cyclic peptide exhibited increased thermal stability compared to the non-cyclic peptides (Fig S1) as expected. For all the type II' turn peptides, an increase in thermal stability of the cyclic peptides was also observed (SI Fig S2). From these results it can be confirmed that CuAAC cyclization of peptides affords stability to β-hairpins regardless of the position of the reaction.

Proteolytic stability of click cyclized β-hairpins

The triazole moiety is known to impart protease resistance as well as is cyclization of a peptide.[18] Thus we sought to test the proteolytic stability of the non-cyclic and cyclic peptides by incubation with Pronase E, which is a mixture of non-specific endo- and exo-serine proteases. The type II' turn sequences were chosen for experimental purposes as it is known that the dPro-Gly turn sequence enhances resistance to protease degradation, thus allowing for measurable half-lives under the conditions.[18] Table 2 summarizes the half-life of each peptide under the conditions described. The β-hairpin peptides were compared to a control unstructured peptide, Scramble, which consisted of a random order of the residues in Term-pG. The half-life of Scramble was found to be 3 minutes, while the non-cyclic peptides HB-pG-U, NHB-pG-U, and Term-pG-U had half-lives of 15, 20, and 60 minutes. The Term-pG-U was found to be the least susceptible to degradation compared to the other non-cyclic peptides, most likely due to being the most well-folded.[18] The CuAAC cyclization improved resistance to proteolytic degradation on all accounts, where HB-pG-C had a half-life 18-fold greater than HB-pG-U, NHB-pG-C showed no observable degradation, and Term-pG-C had a half-life at least 5-fold greater than Term-pG-U and 100-fold greater than Scramble. As the NHB-pG-C peptide did not degrade under the Pronase E conditions, its robustness was also tested using the protease Trypsin which cleaves after the basic amino acids, Arg and Lys. Under trypsin degradation, NHB-pG-C had a half-life of 40 mins which was 4 times greater than the non-cyclic peptide (SI Fig S17 & S18). Additionally, the degradation products were analyzed by mass spectrometry which showed that only the termini were cleaved leaving an intact clicked cycle as the only product. Together these data demonstrate that click cyclization significantly increases protease resistance.

Assessing the ability of clicked β-hairpins to recognize ATP

WKWK binds ATP with a binding constant of 170 μM.[14] The efficacy of the CuAAC peptides to recognize ATP was also assessed for Term and HB peptides as they still contain the necessary Trp-Lys cross-strand pairs for recognition. Term-C and Term-rev-C were determined to have binding constants of 109 uM and 141 uM respectively (Table 3, SI Fig S19). These values do not differ significantly from WKWK. HB-C (K_d = 152 uM) and HB-rev-C (K_d = 267 uM) also bind ATP with comparable affinity. Thus, clicking in these positions has not altered the function of these peptides, providing further support that the overall β-hairpin structure is maintained.

Conclusions

We determined that placing residues compatible for the CuAAC at the terminal ends of a well-folded β-hairpin maintains structure and affords resistance to proteolytic degradation and increased thermal stability. In addition, the function of the peptide is not eliminated and remains comparable to the parent peptide, WKWK. Decreasing the loop size in the cyclic peptide by shortening the azide chain for the terminal position does not impact folding significantly. However, work by Celentano et al. have shown there to be a difference in linker length when the CuAAC participating residues are in the NHB positions.[11]

Cyclizing via the formation of a 1,4-triazole functional group in the non-hyrogen bonded positions improves β-hairpin structure, as evidenced by CD and NMR data. Additionally it can improve solubility as is seen with NHB-rev. In this specific case, Trp9 is sandwiched between the triazole moiety and Lys4; however, this may not be standard to every β-hairpin sequence. The NOESY data clearly indicate that there are more established contacts between the two strands upon cyclization.

Moving the 1,4-triazole to the hydrogen bonded position is most effective in stabilizing the β hairpin structure. This position has intermediate protease stability (SI Fig S11) most likely since there are more residues outside the macrocycle than the other peptides. As in the terminal position, no disruption in binding affinity to ATP is observed.

In summary, the use of the CuAAC reaction afforded an approach to synthesize cyclic β-hairpins in a robust, quick, and high yielding manner that display significant protease resistance while maintaining structure and function. This is a promising approach for producing cyclic β-hairpin peptides for inhibition of protein-protein and protein-nucleic acid interactions.

Experimental

Synthesis and Purification of Peptides

Peptides were synthesized by automated solid-phase peptide synthesis on a Thuramed TetrasUI peptide synthesizer using Fmoc-protected amino acids on CLEAR-amide resin purchased from Peptides International. All natural Fmoc-[N]-protected amino acids were purchased from Advanced Chem Tech. Fmoc-[N]-L-propargyl glycine was purchased from Anaspec and Fmoc-[N]-azidolysine was synthesized from commercially available Fmoc-[N]-Lys-OH from NovaBiochem. Activation of amino acids was performed with HBTU and HOBt in the presence of DIPEA in DMF and NMP. Peptide deprotection was carried out in 2% DBU (1,8-diazobicyclo[5.4.0]undec-7-ene) and 2% piperidine in DMF for 2 cycles of approximately 15 min each. Each coupling step was performed twice for approximately 30 min. All peptides were acetylated at the N-terminus with 5% acetic anhydride and 6% 2,6-lutidene in DMF for 35 min. Cleavage of the peptide from the resin was performed in 95:2.5:2.5 trifluoroacetic acid (TFA): triisopropylsilane (TIPS): water for 3 h. For peptides containing cysteine 94:2.5:2.5:1 trifluoroacetic acid (TFA): ethanedithiol (EDT): TIPS: water was used. TFA was evaporated and cleavage products were precipitated with cold ether. The peptide was extracted into water and lyophilized. It was then purified by reverse-phase HPLC using an Atlantis C-18 semi-preparative column and a gradient of 0 to 100%B over 45 min or 60 min, where solvent A was 95:5 water:acetonitrile with 0.1% TFA and solvent B was 95:5 acetonitrile: water with 0.1% TFA. After purification, the peptide was lyophilized to a powder and identified with ESI-TOF mass spectroscopy.

Synthesis of α-N-Fmoc-ε-azido-L-Lysine.[20]

Fmoc-Lysine-OH (2.7 mmol, 1 eq), potassium carbonate (5.5 mmol, 2 eq), and copper (II) sulfate pentahydrate (0.028 mmol, 1 mol %) were stirred in MeOH (15 mL) for 10 mins. Imidazole-1-sulfonyl azide·HCl (3.3 mmol, 1.2 eq) was then added. [Saftey precaution:

imidazole-1-sulfonyl azide is potentially explosive. Aliquots of less than one gram were stored at 4°C.] This was allowed to react overnight. The reaction mixture was diluted with water (2.5 mL) and the MeOH was removed via rotary evaporation. The reaction was diluted with more water (30 mL) and acidified with HCl (ca. 1 mL). Crude product was extracted into ethyl acetate (3 × 25 mL). The organic layers were combined and dried over $MgSO_4$. Fmoc-Azidolysine-OH was purified by silica gel column chromatography (3–10% MeOH in CH_2Cl_2) to give the desired product as a white solid (80% yield). ^{1}H NMR (400 MHz, CD_3OD): δ 7.69 (d, *J* = 7.6, 2H), δ 7.60 (t, *J* = 8.0, 2H), δ7.31 (t, *J* = 7.2, 2H), δ 7.24 (t, *J* = 7.2, 2H), δ 4.30 (d, *J* = 6.8, 2H), δ 4.19 (m, 1H), δ 4.13 (t,*J* = 6.8, 1H), δ 3.17 (m, 2H), δ 1.90-1.35 (m, 6H)

Synthesis of tris-tri(methylazolyl)amine ligand.[21]

Methylbromoacetate (3.44 mmol, 1 eq) was dissolved in acetone (1.5 mL) and brought to 0°C. Sodium azide (3.56 mmol, 1.03 eq) was dissolved in water (1.5 mL) and slowly added dropwise to the reaction mixture. The mixture was then allowed to warm to room temperature and then heated to 65°C and stirred overnight. Azidomethylacetate was extracted using CH_2Cl_2 (3 × 10 mL). The organic layers were combined and dried over Na_2SO_4. The organics were then rotary evaporated to give azidomethylacetate. Tripropargylamine (0.44 mmol, 1eq) was dissolved in CH_3CN (1 mL) and cooled to −5°C. To this was added azidomethylacetate (1.72 mmol, 3.9 eq) in CH_3CN (1 mL) slowly over 5 mins. 2,6-lutidine (0.44 mmol, 1 eq) and $Cu(MeCN)_4PF_6$ (0.0088 mmol, 2 mol %) was added. The mixture was brought to room temperature then heated to 65°C and allowed to stir for 3 days under a N_2 atmosphere. The CH_3CN was rotary evaporated to dryness. The product was purified by silica gel column chromatography (3 % MeOH in CH_2Cl_2) to give the desired product as an off white solid (82% yield). ^{1}H NMR (400 MHz, $CDCl_3$): δ 7.84 (s, 1H), δ 5.18 (s, 2H), δ 3.79 (s, 2H), δ 3.78 (s, 3H). High-resolution ESI-MS: *m/z* calculated for $C_{18}H_{24}N_{10}O_6$ (M + Cs+), 609.0935; observed 609.0920.

General Procedure for the Cyclization of Peptides using CuAAC

To a solution of peptide (1 mM) in 10 mM phosphate, pH 8.0 buffer was added a premixed solution of tris-tri(methylazolyl)amine ligand (2.7 eq) and $[Cu(CH_3CN)_4][PF_6]$ (1.8 eq) in acetonitrile. Sodium ascorbate (2.1 eq) dissolved in minimal buffer was added to the reaction. This solution was stirred overnight in the dark. The reaction mixture was quenched with %A HPLC solvent and lyophilized to a powder. The reaction was further desalted followed by HPLC purification. The yields were quantitative.

NMR Spectroscopy

NMR samples were made to a concentration of at least 1mM in D_2O buffered to pD 7.0 (uncorrected) with 50 mM KPO_4D_2, 0.5mM DSS. Samples were analyzed on a Varian Inova 600-MHz instrument. One dimensional spectra were collected using 32K data points and between 8 and 36 scans using 1.5 s presaturation. Two dimensional total correlation spectroscopy (TOCSY) and nuclear Overhauser spectroscopy (NOESY) experiments were carried out using the pulse sequences from the Chempack software. Scans in the TOCSY experiment were taken from 16 to 32 in the first dimension and from 64 to 128 in the second

dimension. Scans in the NOESY experiments were taken from 32 to 64 in the first dimension and from 128 to 512 in the second dimension with mixing times of 200–500 ms. All spectra were analyzed using standard window functions (sinbell and Gaussian with shifting). Presaturation was used to suppress the water resonance. Assignments were made by using standard methods as described by Wüthrich.[20] All experiments were run at 298.15K.

Circular Dichroism (CD) spectroscopy

CD spectroscopy was performed on an Applied Photophysics Chirscan Plus. Spectra were collected from 260 to 185 nm at 0.5 nm intervals at 25°C. Melting temperature spectra were collected along the same wavelengths from 25°C to 90°C.

Peptidase Concentration

Enzymes were purchase from Sigma-Aldrich, pronase E from *Streptomyces griseus* (EC 3.4.24.31) as a solid and trypsin from bovine pancrease as a lyophilized powder containing lactose. Pronase E and trypsin were brought up in 10mM sodium phosphate, 140mM NaCl buffer, pH 7.6 to 0.3 mg/mL.

Peptidase Degradation Reactions

The procedure for peptidase studies was adapted from Seebach et al.[21] For each reaction, 0.25 mM peptide in the phosphate buffer (140mM Na^+/K^+Cl^- buffer pH 7.6) was reacted with the appropriate concentration of enzyme at 37°C. A 75 μL aliquot was removed after 0, 5, 10, 15, 30, 45, 60, 90, 120, 190, 270, 360, 480, 600, 720, 840, 1100, 1260, 1440, 1680 min time points, quenched with 10 μL glacial acetic acid and 15 μL of buffer, brining the final volume to 100 μL. A 10 μL aliquot was injected on a Waters Alliance 2695 with an Atlantis C-18 column using a 0–40%B in 45 mins gradient. The acetic acid peak was used as an internal control to account for differences in the injection volumes by the autosampler. The parent peak and the acetic acid peak were integrated using the accompanying software. To determine the fraction of full-length peptides remaining at each of the time points, the peak area for the full-length peptides was divided by the peak are at the zero time point.

Fluorescence Quenching Experiments with ATP

Peptide samples were prepared by dissolving purified peptide in 10 mM acetate buffer, pH 5.0. The concentrations of the peptide was determined in 5M guanidine hydrochloride using the absorbance of the Trp residues at 280 nm ($\varepsilon = 5690\ M^{-1}\ cm^{-1}$). An ATP stock solution was prepared by dissolving in 10 mM acetate buffer, pH 5.0, and the concentration was determined using the absorbance at 260 nm ($\varepsilon = 15400\ M^{-1}\ cm^{-1}$). ATP concentrations were prepared via serial dilutions. Samples were prepared where the peptide host concentrations were held constant with increasing concentrations of guest. Fluorescence scans were obtained at 25°C using an excitation wavelength of 297 nm for Trp. Emission was monitored between at 348 nm. The emission intensities of Trp at 348 nm as a function of nucleotide concentration were fit to this binding equation in

$$I = \frac{I_0 + I_8 \frac{[L]}{K_d}}{1 + \frac{[L]}{K_d}}$$

Kaleidagraph, where I is the observed fluorescence intensity, I_0 is the initial intensity, I_8 is the fluorescence intensity at binding saturation, [L] is the concentration of ATP added, and K_d is the dissociation constant.

Supplementary Material

Refer to Web version on PubMed Central for supplementary material.

Notes and references

1. (a) Chene P. Nat Rev Cancer. 2003; 3:102–109. [PubMed: 12563309] (b) Klein C, Vassilev LT. British Journal of Cancer. 2004; 91:1415–1419. [PubMed: 15452548]
2. Puigserver P. Age. 2007; 29:115–115.
3. (a) Rodgers JT, Lerin C, Haas W, Gygi SP, Spiegelman BM, Puigserver P. Nature. 2005; 434:113–118. [PubMed: 15744310] (b) Billia F, Hauck L, Konecny F, Rao V, Shen J, Mak TW. Proc Nat Acad Sci USA. 2011; 108:9572–9577. [PubMed: 21606348] (c) Manolov DE, Koenig W, Hombach V, Torzeski J. Histology and Histopathology. 2003; 18:1189–1193. [PubMed: 12973687]
4. (a) Robinson JA. Chembiochem. 2009; 10:971–973. [PubMed: 19266524] (b) Wilson AJ. Chem Soc Rev. 2009; 38:3289–3300. [PubMed: 20449049]
5. (a) Walensky LD, Kung AL, Escher I, Malia TJ, Barbuto S, Wright RD, Wagner G, Verdine GL, Korsmeyer SJ. Science. 2004; 305:1466–1470. [PubMed: 15353804] (b) Torres O, Yuksel D, Bernardina M, Kumar K, Bong D. Chembiochem. 2008; 9:1701–1705. [PubMed: 18600813] (c) Empting M, Avrutina O, Meusinger R, Fabritz S, Reinwarth M, Biesalski M, Voigt S, Buntkowsky G, Kolmar H. Angew Chem Int Ed Engl. 2011; 50:5207–5211. [PubMed: 21544910] (d) Scrima M, Le Chevalier-Isaad A, Rovero P, Papini AM, Chorev M, D'Ursi AM. Euro J Org Chem. 2010:446–457.
6. Moellering RE, Cornejo M, Davis TN, Del Bianco C, Aster JC, Blacklow ALK, Gilliland DG, Verdine GL, Bradner JE. Nature. 2009; 462:182–190. [PubMed: 19907488]
7. Henchey LK, Kushal S, Dubey R, Chapman RN, Olenyuk BZ, Arora PS. J Am Chem Soc. 2010; 132:941–943. [PubMed: 20041650]
8. (a) Rostovtsev VV, Green LG, Fokin VV, Sharpless KB. Angew Chem Int Ed Engl. 2002; 41:2596–2599. [PubMed: 12203546] (b) Tornoe CW, Christensen C, Meldal M. J Org Chem. 2002; 67:3057–3064. [PubMed: 11975567]
9. Jacobsen O, Maekawa H, Ge NH, Gorbitz CH, Rongved P, Ottersen OP, Amiry-Moghaddam M, Klaveness J. J Org Chem. 2011; 76:1228–1238. [PubMed: 21275402]
10. Holland-Nell K, Meldal M. Angew Chem Int Ed Engl. 2011; 50:5204–5206. [PubMed: 21472909]
11. Celentano V, Diana D, De Rosa L, Romanelli A, Fattorusso R, D'Andrea LD. Chem Commun. 2011; 48:762–764.
12. (a) White CJ, Yudin AK. Nat Chem. 2011; 3:509–524. [PubMed: 21697871] (b) Li P, Roller PP, Xu J. ChemInform. 2003; 34:411–440.
13. (a) Fasan R, Dias RLA, Moehle K, Zerbe O, Obrecht D, Mittle PRE, Grütter MG, Robinson JA. ChemBioChem. 2006; 7:515–526. [PubMed: 16511824] (b) Moehle K, Athanassiou Z, Patora K, Davidson A, Varani G, Robinson JA. Angew Chem Int Ed. 2007; 46:9101–9108.
14. (a) Butterfield SM, Waters ML. J Am Chem Soc. 2003; 125:9580–9581. [PubMed: 12904011] (b) Butterfield SM, Sweeney MM, Waters ML. J Org Chem. 2005; 18:1105–1114. [PubMed: 15704942]

15. (a) Angell YL, Burgess K. Chem Soc Rev. 2007; 36:1674–1689. [PubMed: 17721589] (b) Empting M, Avrutina O, Meusinger R, Fabritz S, Reinwarth M, Biesalski M, Voigt S. Angew Chem Int Ed. 2011; 50:5207–5211.(c) Ingale S, Dawson PE. Org Lett. 2011; 13:2822–2825. [PubMed: 21553819]

16. Hughes, RM. Doctoral dissertation. University of North Carolina; 2007. Non-covalent interactions in β-hairpin peptides and small molecule model systems.

17. Syud FA, Espinosa JF, Gellman SH. J Am Chem Soc. 1999; 121:11577–11578.

18. Jochim AL, Miller SE, Angelo NG, Arora PS. Bioorg Med Chem Lett. 2009; 19:6023–6026. [PubMed: 19800230]

19. Cline LL, Waters ML. Peptide Science. 2009; 92:502–507. [PubMed: 19521977]

20. (a) Mahmoud ZN, Gunnoo SB, Thomson AR, Fletcher JM, Woolfson DN. Biomaterials. 2011; 32:3712–3720. [PubMed: 21353303] (b) Isaad ALC, Barbetti F, Rovero P, D'Ursi AM, Chelli M, Chorev M, Papini AM. Eur J Org Chem. 2008; 31:5308–5314.(c) Cantel S, Isaad ALC, Scrima M, Levy JJ, DiMarchi RD, Rovero P, Halperin JA, D'ursi AM, Papini AM, Chorev MJ. Org Chem. 2008; 73:5663–5674.

21. a) Chan TR, Hilgraf R, Sharpless KB, Fokin VV. Org Lett. 2004; 6:2853–2855. [PubMed: 15330631] (b) Juricek M, Stout K, Kouwer PHJ, Rowan AE. Org Lett. 2011; 13:3494–3497. [PubMed: 21648454]

22. Wüthrich, K. NMR of Proteins and Nucleic Acids. New York: Wiley; 1986.

23. Frackenpohl J, Arvidsson PI, Schreiber JV, Seebach D. ChemBioChem. 2001; 2:445–455. [PubMed: 11828476]

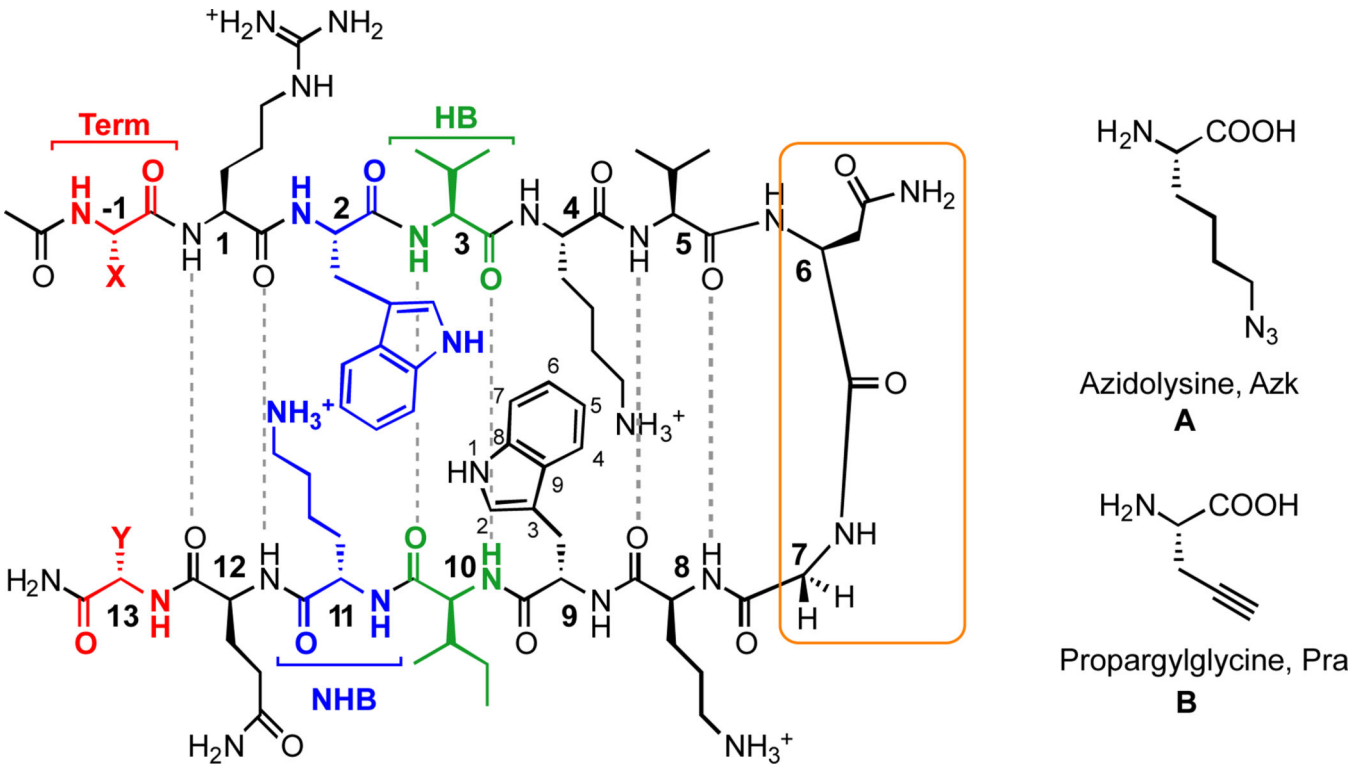

Fig. 1.

Peptides investigated for CuAAC hairpin cyclization. The functional amino acids for CuAAC, **A** and **B**, are varied along terminal (Term, red), non-hydrogen bonded (NHB, blue), and hydrogen bonded (HB, green) positions. The turn residues (orange) can be one of two sequences, VNGO (shown) or VpGO, where p = dPro. Dashed lines represent hydrogen bonds.

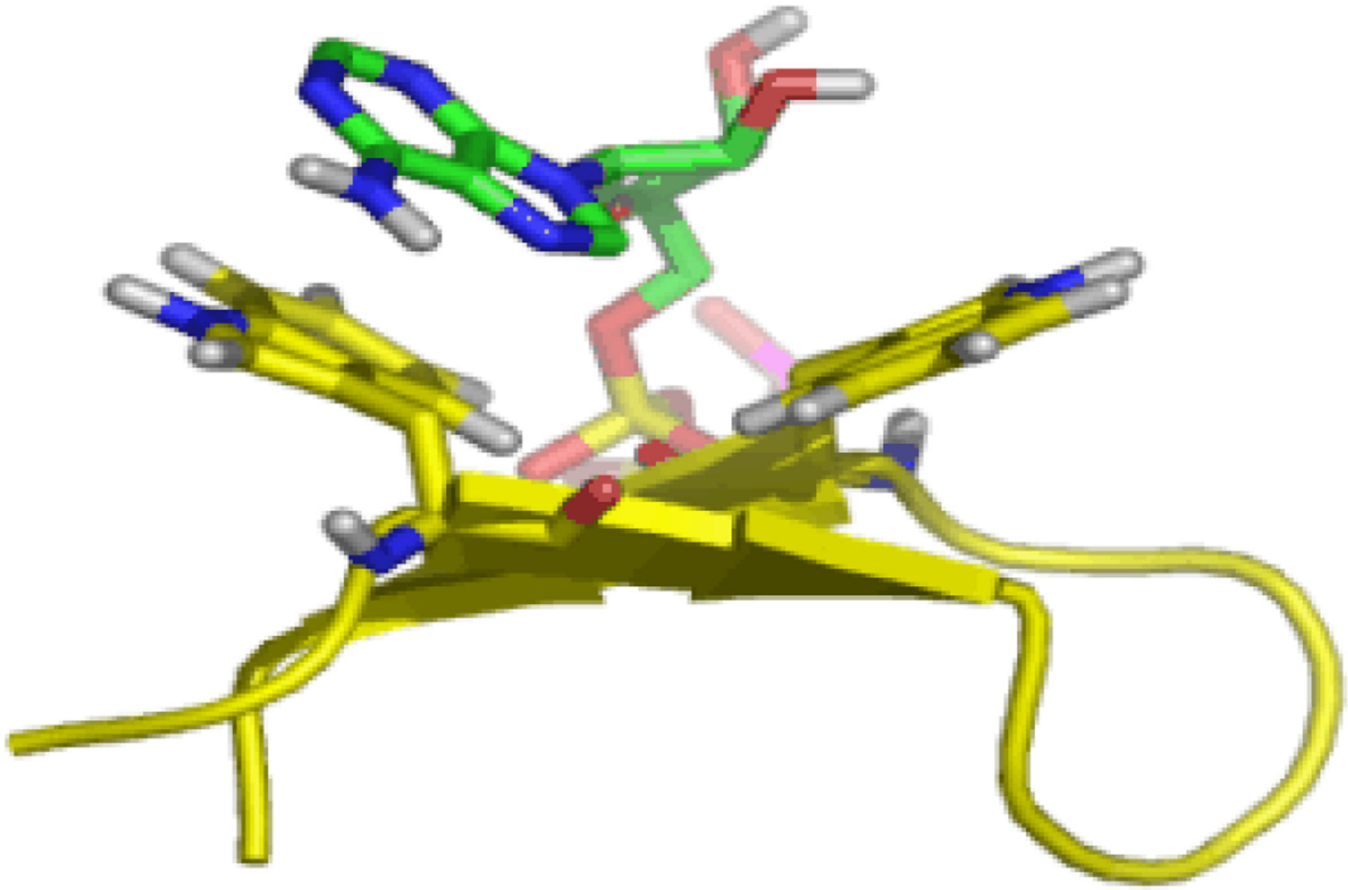

Fig. 2.

Molecular dynamics simulation of WKWK (yellow) with the Trp shown in stick form bound to ATP (green).[16] The peptide structure is based on an NMR structure.

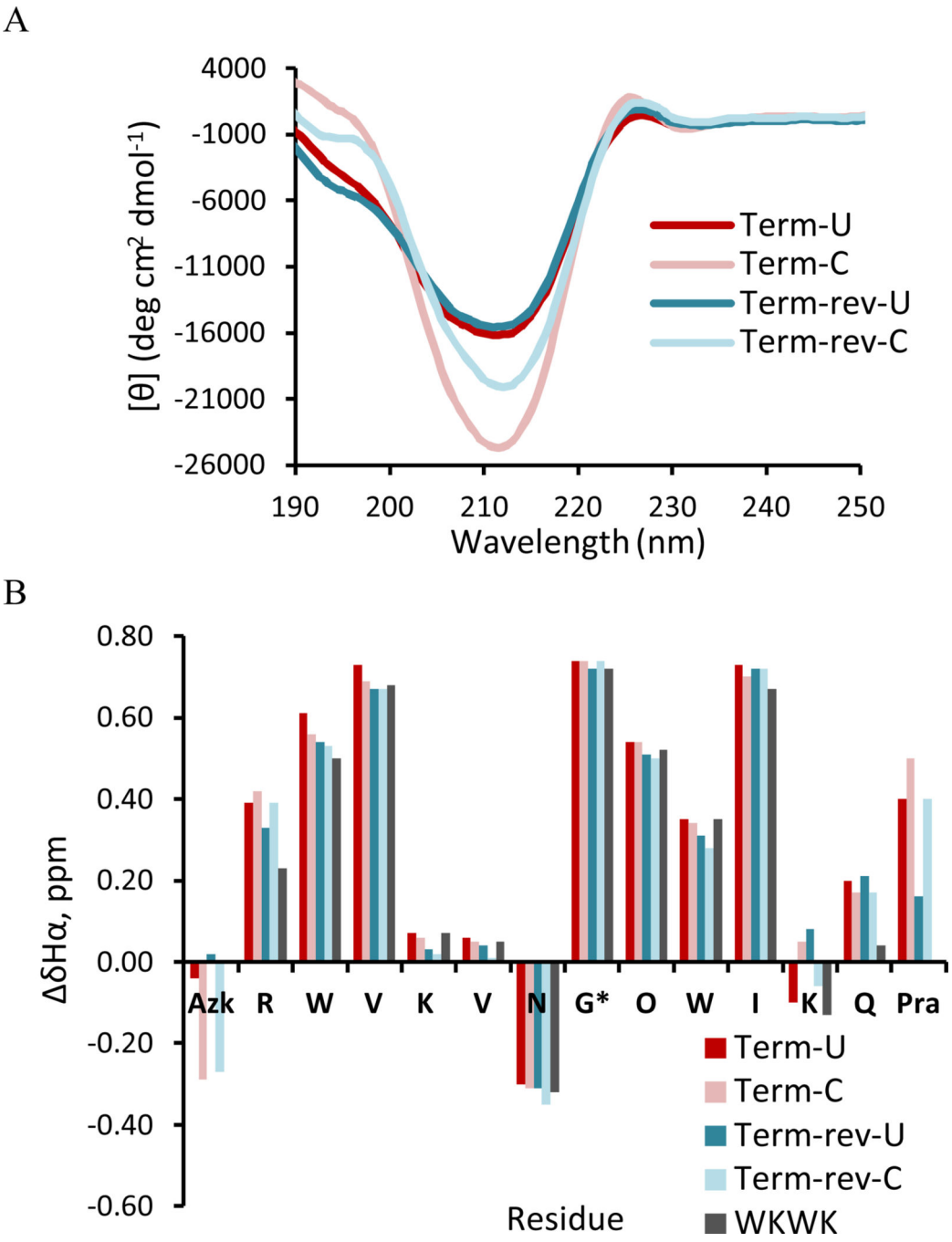

Fig. 3.

(A) Circular dichroism spectra for terminal position peptides. 50 μM peptide in 10 mM sodium phosphate buffer, pH 7.4. (B) Chemical shift differences of Hα for terminal position peptides. Values for Gly* are glycine splitting values. TOCSY data were acquired with peptide concentrations at 1 mM in 50 mM KD_2PO_4, pH 7 buffer at 20 °C.

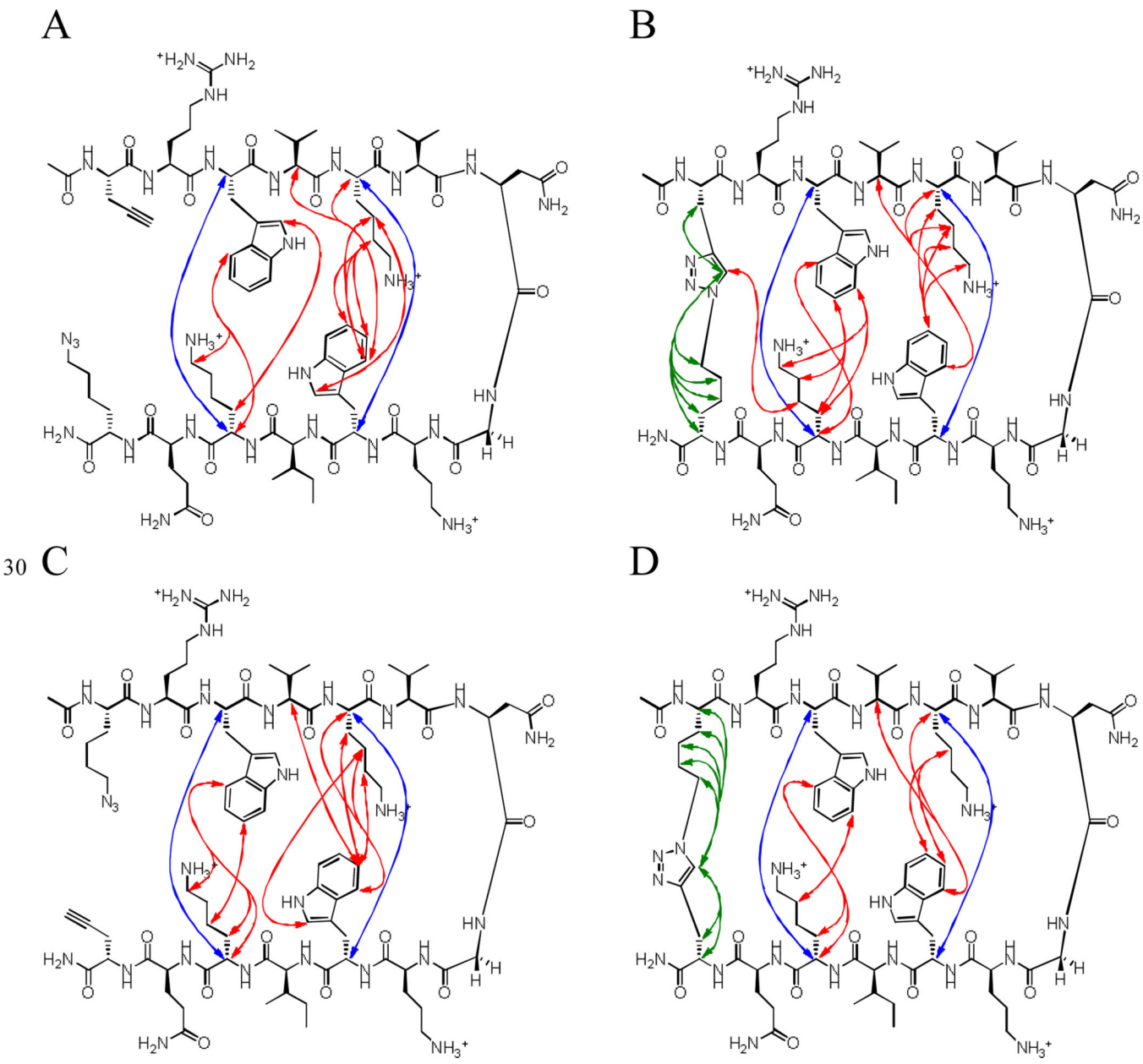

Fig. 4.

Unambiguous NOEs seen for A) Term-U, B) Term-C, C) Term-rev-U, D) Term-rev-C Shown are cross strand interactions (blue) confirming registry, triazole interactions (green), and residue interactions (red). NOESY spectra were acquired with peptide concentration around 1 mM in 50 mM KD_2PO_4, pH 7 buffer at 20 °C.

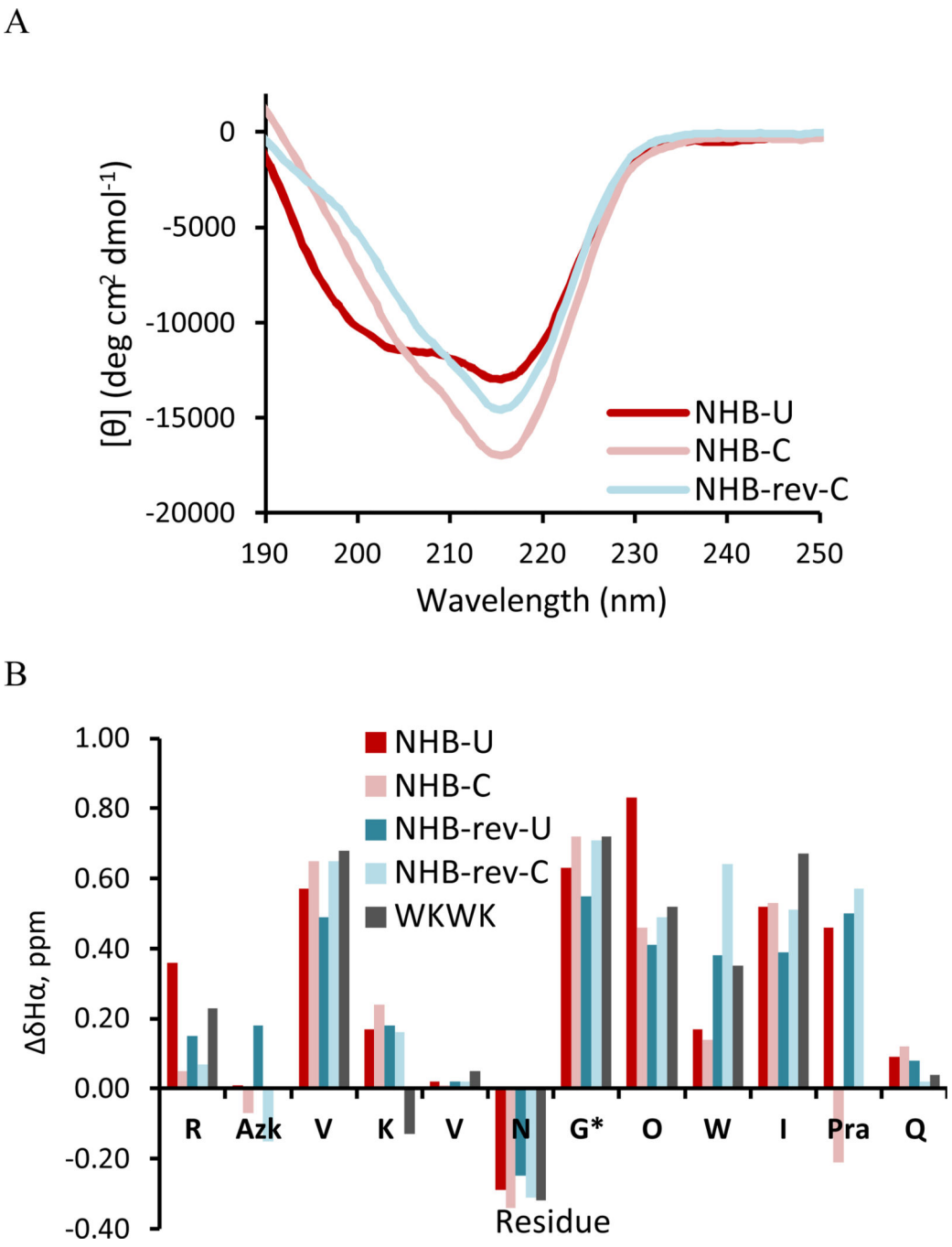

Fig. 5.

(A) Circular dichroism spectra for non-hydrogen bonded position peptides. 50 μM peptide in 10 mM sodium phosphate buffer, pH 7.4. (B) Chemical shift differences of Hα for non-hydrogen bonded position peptides. Values for Gly* are glycine splitting values. TOCSY data were acquired with peptide concentrations at 1 mM in 50 mM KD_2PO_4, pH 7 buffer at 20 °C with the exception of NHB-rev-U which was acquired in a 50 mM *d*-acetate buffer, pH 4.0.

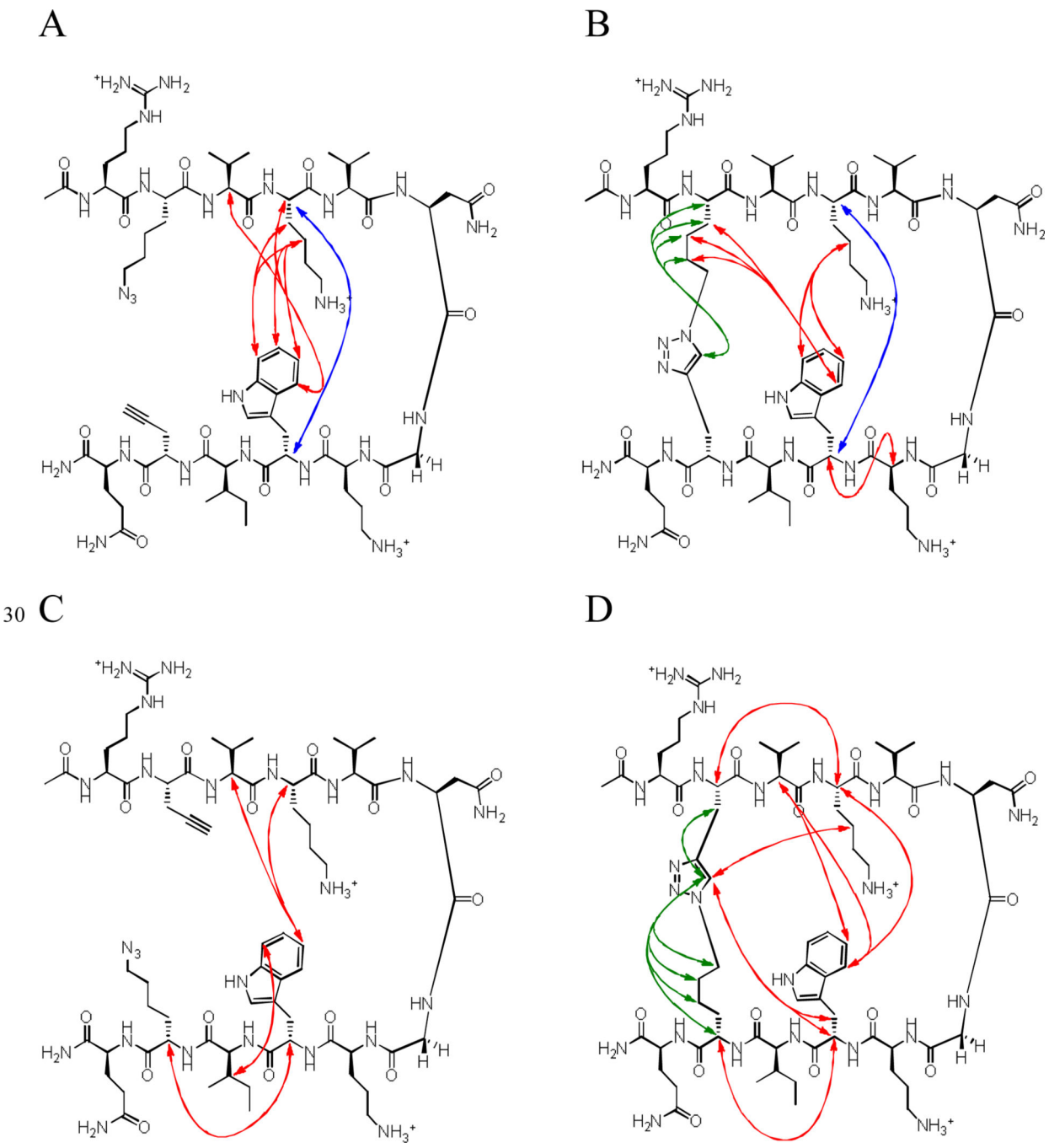

Fig. 6.

Unambiguous NOEs seen for A) NHB-U, B) NHB-C, C) NHB-rev-U, D) NHB-rev-C Shown are cross strand interactions (blue) confirming registry, triazole interactions (green), and residue interactions (red). NOESY spectra were acquired with peptide concentration around 1 mM in 50 mM KD_2PO_4, pH 7 buffer at 20 °C with the exception of NHB-rev-U which was acquired in a 50 mM *d*-acetate buffer, pH 4.0.

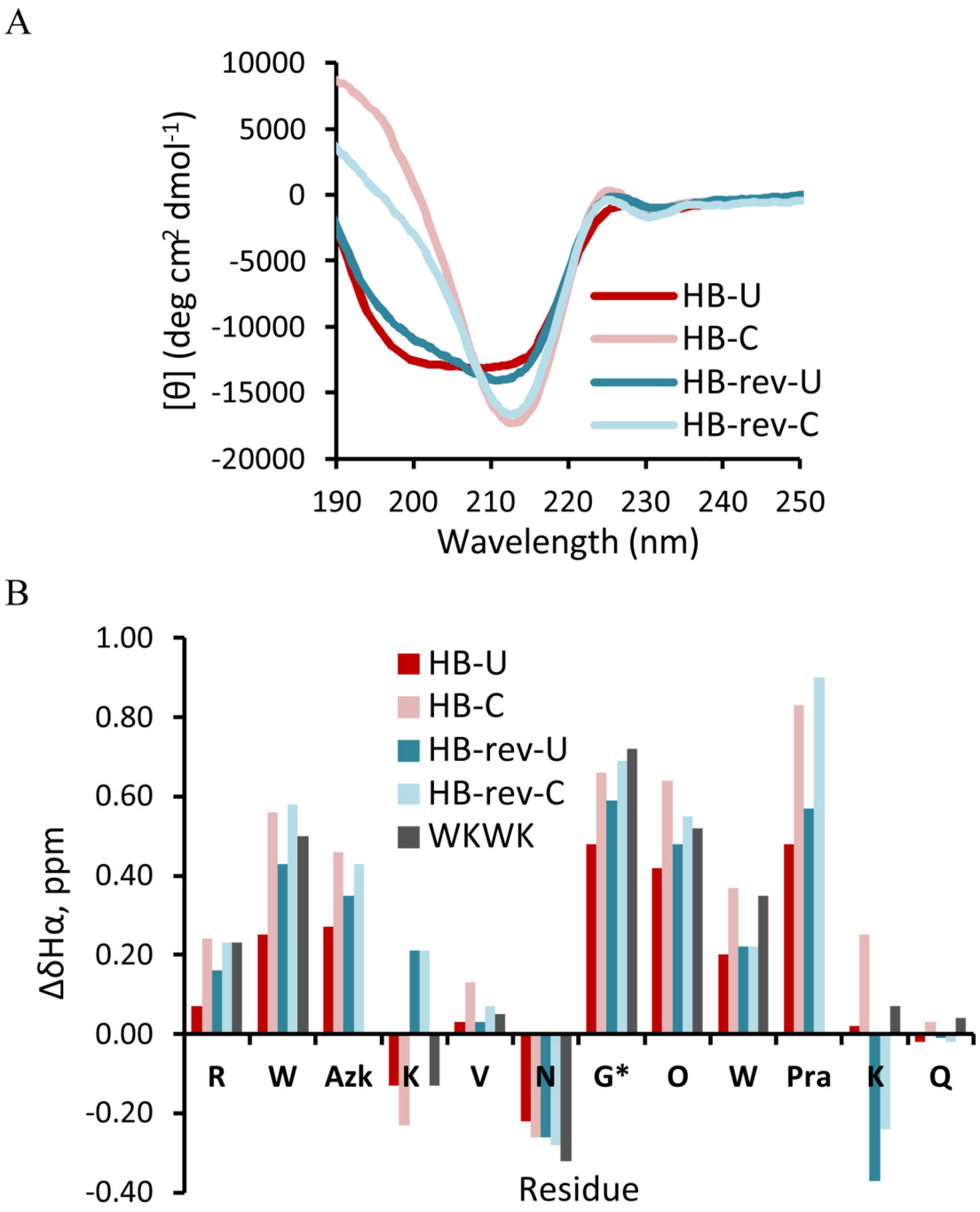

Fig. 7.

(A) Circular dichroism spectra for hydrogen bonded position peptides. 50 μM peptide in 10 mM sodium phosphate buffer, pH 7.4. (B) Chemical shift differences of Hα for hydrogen bonded position peptides. Values for Gly* are glycine splitting values. TOCSY data were acquired with peptide concentrations at 1 mM in 50 mM KD_2PO_4, pH 7 buffer at 20 °C.

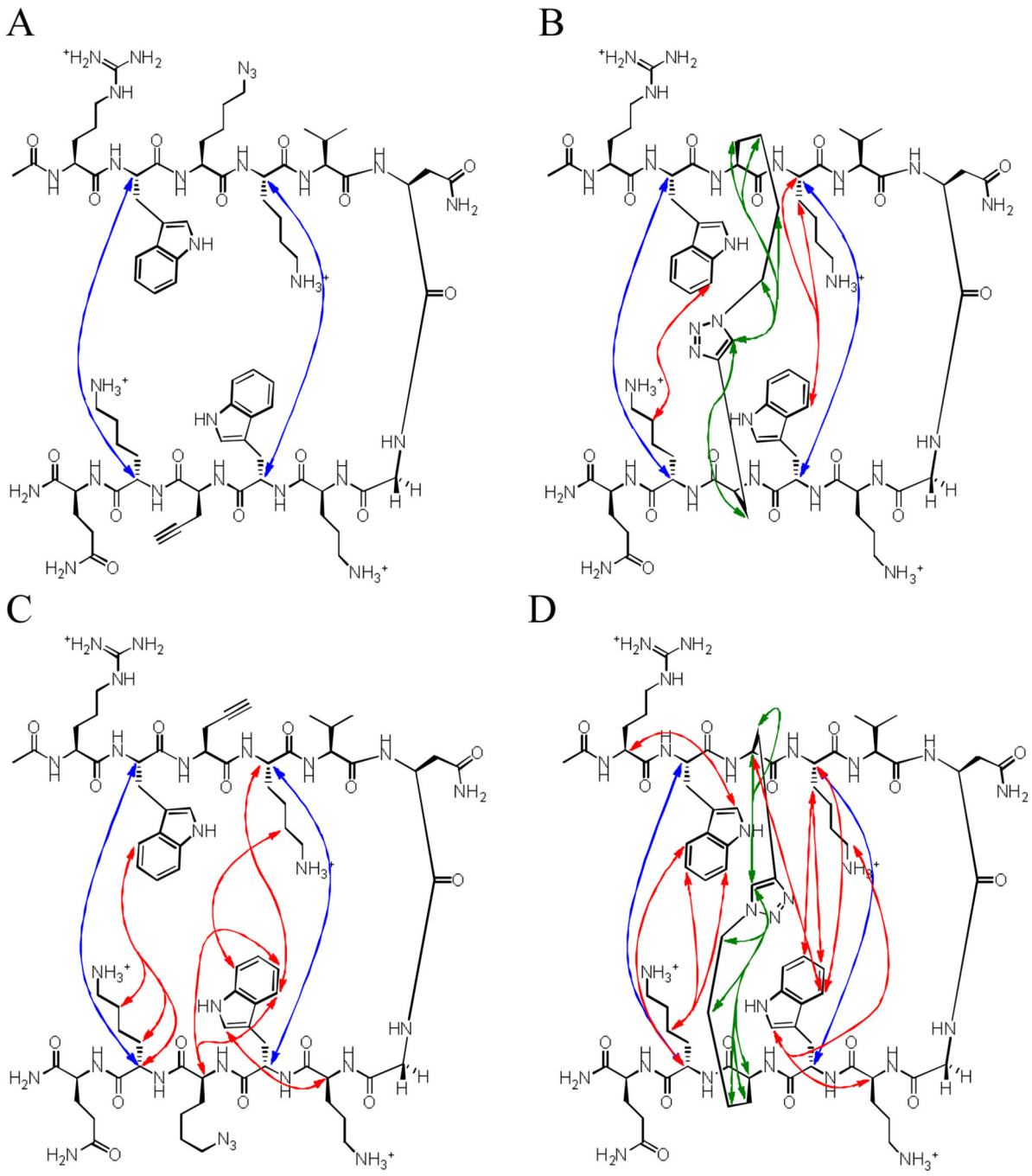

Fig. 8.

Unambiguous NOEs seen for A) HB-U, B) HB-C, C) HB-rev-U, D) HB-rev-C Shown are cross strand interactions (blue) confirming registry, triazole interactions (green), and residue interactions (red). NOESY spectra were acquired with peptide concentration around 1 mM in 50 mM KD_2PO_4, pH 7 buffer at 20 °C.

Table I

Sequence of β-hairpin peptides

Peptide	Sequence
WKWK	Ac-R**W**V**K**VNGO**W**I**K**Q-NH_2
Term	Ac-(Azk)R**W**V**K**VNGO**W**I**K**Q(Pra)-NH_2
Term- rev	Ac-(Pra)R**W**V**K**VNGO**W**I**K**Q(Azk)-NH_2
NHB	Ac-R(Azk)VKVNGOWI(Pra)Q-NH_2
NHB-rev	Ac-R(Pra)VKVNGOWI(Azk)Q-NH_2
HB	Ac-R**W**(Azk)**K**VNGO**W**(Pra)**K**Q-NH_2
HB-rev	Ac-R**W**(Pra)**K**VNGO**W**(Azk)**K**Q-NH_2
Term-pG	Ac-(Azk)RWVKVpGOWIKQ(Pra)-NH_2
NHB-pG	Ac-R(Azk)VKVpGOWI(Pra)Q-NH_2
HB-pG	Ac-RW(Azk)KVpGOW(Pra)KQ-NH_2

Residues involved in turn sequence are underlined. Residues involved in potential ATP recognition are in bold. Prefixes of “U” and “C” denote linear unclicked and cyclic clicked peptides. p = dPro.

Table 2

Half-lives of type II' turn peptides treated with Pronase E*

	$t_{1/2}$ (min)	
Peptide	**U**	**C**
Scramble**	3 (± 5)	--
HB-pG	15 (± 5)	280 (± 5)
NHB-pG	20 (± 5)	No observable degradation***
Term-pG	60 (± 5)	> 300

* Reactions carried out in 10 mM sodium phosphate, 140 mM NaCl, pH 7.6 with 500 μM peptide at 37 °C.

** Scrambled sequence: Ac-pQVIKRGOWW(Pra)(AzK)VK-NH_2

*** Over a 48 hour time period

Table 3

Binding Constants of Peptides for ATP

Peptide	K_d, μM (error)
WKWK	170
Term-C	110 (30)
Term-rev-C	140 (20)
HB-C	150 (20)
HB-rev-C	270 (20)